2020 IEEE International Conference on Robotics and Automation (ICRA)
31 May - 31 August, 2020. Paris, France

Trajectory Planning with Safety Guaranty for a Multirotor based on the Forward and Backward Reachability Analysis

Hoseong Seo, Clark Youngdong Son, Dongjae Lee, and H. Jin Kim

***Abstract*— Planning a trajectory with guaranteed safety is a core part for a risk-free flight of a multirotor. If a trajectory planner only aims to ensure safety, it may generate trajectories which overly bypass risky regions and prevent the system from achieving specific missions. This work presents a robust trajectory planning algorithm which simultaneously guarantees the safety and reachability to the target state in the presence of unknown disturbances. We first characterize how the forward and backward reachable sets (FRSs and BRSs) are constructed by using Hamilton-Jacobi reachability analysis. Based on the analysis, we present analytic expressions for the reachable sets and then propose minimal ellipsoids which closely approximate the reachable sets. In the planning process, we optimize the reference trajectory to connect the FRSs and BRSs, while avoiding obstacles. By combining the FRSs and BRSs, we can guarantee that any state inside of the initial set reaches the target set. We validate the proposed algorithm through a simulation of traversing a narrow gap.**

I. Introduction

Safety guarantee is a key feature for employing a wide range of applications with multirotor systems. Motivated by the importance of safety, various recent works on trajectory planning for multirotors have focused on producing a safe flight path in complex environments. However, determining in advance whether the planned trajectory will be safe during runtime is a challenging problem, since a multirotor is susceptible to unavoidable disturbances. Those disturbances are usually unknown and have a nonlinear effect on the dynamics, therefore, trajectory tracking error must occur even though a robust controller attempts to reject disturbances.

The objective of this paper is to plan a trajectory which ensures safety and reachability to the target set simultaneously as illustrated in Fig. 1. We concentrate on a less conservative and mission-oriented robust trajectory planning, considering that the trajectory planning to ensure only safety can be overly conservative. It prevents the system from accomplishing specific missions such as passing through a narrow window. We also emphasize that the robust flight trajectory must be computed sufficiently fast, since the multirotor may encounter additional disturbances which exceed the pre-set bounds. For this purpose, we analyze the reachable sets using the Hamilton-Jacobi reachability analysis [1] and propose compact ellipsoidal approximation on the reachable sets. Then, we formulate a tractable trajectory optimization problem based on the ellipsoidal reachable sets. The optimization aims to connect the forward and backward reachable sets (FRSs and BRSs) while avoiding obstacles. All of the states inside of the initial set are guaranteed to reach the target set when the FRSs enter the BRSs. Consequently, the proposed method can ensure safety and reachability to the target set.

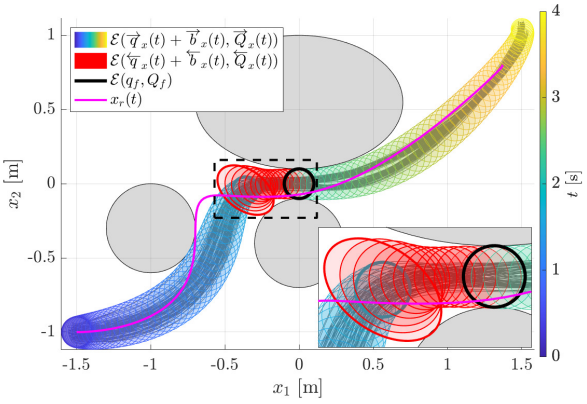

Fig. 1. Illustrative simulation for the multirotor passing through between obstacles. Colored regions are the forward reachable sets over time, which start with blue and end with yellow. The magenta line is the planned reference trajectory. The thick black line is the boundary of the target set, and red regions are the corresponding backward reachable sets. Shaded grey regions are obstacles. Gray trajectories inside of the colored regions are the reference tracking results starting from the randomly sampled initial states. Planning with the backward reachable sets generates the reference trajectory which can traverse the complex region without collision. Symbolic notations will be explained in Sec. IV.

A. Related Works

The sum-of-squares (SOS) programming is used to compute the safety funnels. [2] computes the funnels around a finite number of predefined motion primitives in the offline phase. In the online optimization, duration and sequence of the funnels are determined such that the overall trajectory is collision-free. [3] presents the funnel library for the closed-loop dynamics of the multirotor system. The funnels are computed for various disturbance bounds in the offline phase and then combined during the online phase. The main drawback of those approaches is a heavy computation load for the offline phase. When some system parameters such as mass, controller gains, or disturbance bounds are changed, the funnel library must be recomputed, and it is difficult to swiftly react to those sudden changes.

The SNU-Samsung smart campus research center (0115-20190023) at Seoul National University provides research facilities for this study. And, this material is based upon work supported by the Ministry of Trade, Industry & Energy(MOTIE, Korea) under Industrial Technology Innovation Program (No. 10051673).

Hoseong Seo is with the Automation and Systems Research Institute and Department of Mechanical and Aerospace Engineering, Seoul National University, Seoul, South Korea. hosung37@snu.ac.kr

Clark Youngdong Son and Dongjae Lee are with the Department of Mechanical and Aerospace Engineering, Seoul National University, Seoul, South Korea. {clark.y.d.son, ehdwo713}@snu.ac.kr

H. Jin Kim is with the Institute of Engineering Research and Department of Mechanical and Aerospace Engineering, Seoul National University, Seoul, South Korea. hjinkim@snu.ac.kr

A different class of works formulates a robust trajectory planning problem as a two-player game between planning and tracking systems. [4] computes the maximum possible tracking error between the planning and tracking systems using the Hamilton-Jacobi (HJ) reachability analysis during the offline phase. As an extended version of the work above, [5] considers various types of planning systems and perform the reachability analysis for each planning model. Similar to the case of the funnel library, this class of methods requires reevaluation on the reachable sets when system parameters are changed.

Tube-based model predictive control (TMPC) techniques attempt to compute the reachable sets online. [6] and [7] compute the robust forward invariant tubes and the optimal control inputs at the same time for a receding horizon based on differential inequalities. Those invariant tubes require the solution of a matrix-valued differential equation. [8] proposes an approximation on the disturbance invariant sets, but it requires numerical propagation of all the states in the initial set and provides no theoretical guarantee on the safety.

B. Contributions

- **Computational simplicity**: The proposed reachable set computation does not need any optimization. Thus, it is computationally efficient compared to most of the other works which require numerical optimization.
- **Safety and performance guarantee**: By composing the forward and backward reachable sets in planning trajectory, our method can guarantee the reachability to the target set while ensuring the safety of the system.

C. Outline

Section II describes the problem we want to solve. Section III details the computation of the reachable sets as ellipsoids. Section IV provides the simulation results of the proposed planning algorithm. Section V concludes the paper.

II. Problem Formulation

A. System Dynamics

We consider the following simplified multirotor dynamics:

$$\dot{x}(t) = f\big(x(t),u(t),w(t)\big),$$
$$\begin{cases} \dot{\mathbf{p}} & = \mathbf{v} \\ m\dot{\mathbf{v}} & = FR(\Phi)e_3 + m\mathbf{g} + \Delta\,, \\ \dot{\Phi} & = G(\Phi)\omega \end{cases}$$

where $\mathbf{p} \in \mathbb{R}^3$ and $\mathbf{v} \in \mathbb{R}^3$ are the position and velocity expressed in the inertial frame, $\Phi \in \mathbb{R}^3$ is the Euler angles, $R \in \mathbb{R}^{3\times3}$ is the rotation matrix, $F \in \mathbb{R}$ is the total thrust, $\omega \in \mathbb{R}^3$ is the angular velocity, $G \in \mathbb{R}^{3\times3}$ is the mapping between the rates of the Euler angles and the angular velocity, $\mathbf{g} \in \mathbb{R}^3$ is the gravitational acceleration, $m \in \mathbb{R}$ is the total mass, $\Delta \in \mathbb{R}^3$ is the external force disturbance, and $e_3 = [0\,0\,1]^\top$. State and input vectors are $x = [\mathbf{p}^\top\,\mathbf{v}^\top\,\Phi^\top]^\top \in \mathbb{R}^{n_x}$ and $u = [F\,\omega^\top]^\top \in \mathbb{R}^{n_u}$, where $n_x = 9$ and $n_u = 4$. We utilize the geometric controller [9] summarized as

$$u(t) = \mu(x(t),x_r(t),w(t);K(t)),$$

where $x_r \in \mathbb{R}^9$ is the reference state which is a stack of reference position, velocity and acceleration vectors. The controller has position, velocity, and rotation feedback gains $K \in \mathbb{R}^9$ as parameters. We also consider state measurement noise $\delta\mathbf{p} \in \mathbb{R}^3$, $\delta\mathbf{v} \in \mathbb{R}^3$ and $\delta\Phi \in \mathbb{R}^3$ as disturbances. So, the disturbance vector is $w = [\delta\mathbf{p}^\top\,\delta\mathbf{v}^\top\,\delta\Phi^\top\,\Delta]^\top \in \mathbb{R}^{n_w}$, where $n_w = 12$. The closed-loop dynamics can be written as

$$\begin{aligned}\dot{x}(t) &= f\big(x(t),\mu(x(t),x_r(t),w(t)),w(t)\big) \\ &= g\big(x(t),x_r(t),w(t)\big)\end{aligned} \tag{1}$$

B. Forward and Backward Reachable Sets

Let us denote a set of states at time t as $\mathcal{X}(t) \subset \mathbb{R}^{n_x}$. The forward reachable set $\vec{\mathcal{X}}(t_0,t) \subset \mathbb{R}^{n_x}$ is the set of states at t starting from an initial set of states $\mathcal{X}(t_0)$ in the presence of disturbances [10]. The definition of the FRS is

$$\vec{\mathcal{X}}(t_0,t) = \left\{ a \,\middle|\, \begin{array}{l} \forall\tau \in [t_0,t],\ \exists w(\tau) \in \mathbb{W}, \\ \dot{x}(\tau) = g\big(x(\tau),x_r(\tau),w(\tau)\big), \\ x(t_0) \in \mathcal{X}(t_0),\ a = x(t) \end{array} \right\},$$

where $\mathbb{W} \subset \mathbb{R}^{n_w}$ is an admissible convex set for disturbances. Similarly, the backward reachable set $\overleftarrow{\mathcal{X}}(t,t_f) \subset \mathbb{R}^{n_x}$ is the set of states at t guaranteed to arrive in a target set of states $\mathcal{X}(t_f)$, considering all possible disturbances [10]. Mathematically, the BRS is defined as

$$\overleftarrow{\mathcal{X}}(t,t_f) = \left\{ a \,\middle|\, \begin{array}{l} \forall\tau \in [t,t_f],\ \forall w(\tau) \in \mathbb{W}, \\ \dot{x}(\tau) = g\big(x(\tau),x_r(\tau),w(\tau)\big), \\ x(t_f) \in \mathcal{X}(t_f),\ a = x(t) \end{array} \right\}.$$

The objective of the Hamilton-Jacobi reachability analysis is to find the value function $V(x,t)$ whose subzero level set represents the reachable set [1] expressed as

$$\vec{\mathcal{X}}(t_0,t) = \big\{a | V^{FRS}(a,t) \le 0\big\},$$
$$\overleftarrow{\mathcal{X}}(t,t_f) = \big\{a | V^{BRS}(a,t) \le 0\big\}.$$

We define a convex initial value function $l_0(x)$ which satisfies $\mathcal{X}(t_0) = \{a | l_0(a) \le 0\}$. From the dynamic programming principle [11], the value function $V^{FRS}(x,t)$ is the solution of the initial value HJ partial differential equation (PDE):

$$\begin{cases} \dfrac{\partial V^{FRS}}{\partial t} + H^{FRS}\left(x, \dfrac{\partial V^{FRS}}{\partial x}, t\right) = 0 \\ V^{FRS}(x,t_0) = l_0(x) \\ H^{FRS}(x,p,t) = \max\limits_{w\in\mathbb{W}} \big(p \cdot \dot{x}(t)\big) \end{cases}. \tag{2}$$

See [10], [12] for more detailed explanation on the forward reachability problem. In the case of the backward reachability, we introduce a convex final value function $l_f(x)$ which satisfies $\mathcal{X}(t_f) = \{a | l_f(a) \le 0\}$. Similarly, the value function $V^{BRS}(x,t)$ is determined from the final value HJ PDE:

$$\begin{cases} \dfrac{\partial V^{BRS}}{\partial t} + H^{BRS}\left(x, \dfrac{\partial V^{BRS}}{\partial x}, t\right) = 0 \\ V^{BRS}(x,t_f) = l_f(x) \\ H^{BRS}(x,p,t) = \min\limits_{w\in\mathbb{W}} \big(p \cdot \dot{x}(t)\big) \end{cases}. \tag{3}$$

We assume that each channel of the disturbance is

bounded, i.e. $\underline{w}_i \le w_i(\tau) \le \bar{w}_i$ for all $\tau \in [t_0, t_f]$, where $\underline{w}$ and $\bar{w} \in \mathbb{R}^{n_w}$ are the lower and upper bounds, and the subscript i represents the i-th element of a vector. So, we consider the set for disturbances $\mathbb{W}$ as a hyperrectangle whose center is $w_m = \frac{1}{2}(\bar{w} + \underline{w})$ and length of edge is $w_M = \frac{1}{2}(\bar{w} - \underline{w})$.

C. Problem Statement

We formulate the following trajectory planning problem:

$$\begin{aligned} \min_{x_r(t)} \quad & \int_{t_0}^{t_f} L(x_r(\tau))\, d\tau \\ \text{s.t} \quad & \mathcal{X}(t_0) = \mathcal{X}_0, \quad c(\vec{\mathcal{X}}(t_0,\tau)) > 0 \quad \forall \tau \in [t_0, t_c], \\ & \mathcal{X}(t_f) = \mathcal{X}_f, \quad c(\overleftarrow{\mathcal{X}}(\tau, t_f)) > 0 \quad \forall \tau \in [t_c, t_f], \\ & \vec{\mathcal{X}}(t_0, t_c) \subset \overleftarrow{\mathcal{X}}(t_c, t_f), \end{aligned} \tag{4}$$

where L is the stage cost function related with the reference trajectory, $\mathcal{X}_0 \subset \mathbb{R}^{n_x}$ is the given initial set of states, $\mathcal{X}_f \subset \mathbb{R}^{n_x}$ is the target set of states we want to reach, c represents the nonlinear constraints for collision avoidance, and t_c is the time between t_0 and t_f. Note that the constraints described in the first two lines ensure that the system can avoid obstacles whenever disturbance does not exceed the bound. We propagate the FRSs before t_c and the BRSs after t_c, therefore, the last constraint guarantees that any state in $\mathcal{X}_0$ can reach $\mathcal{X}_f$. We set t_c as a value near t_f, since the backward reachable set far from t_f may not exist.

The trajectory optimization (4) is not a tractable problem in the present form. Every time we update $x_r(t)$ during the optimization, the forward and backward reachable sets must be recomputed because the closed-loop dynamics (1) is also changed according to the updated reference. Furthermore, solving PDEs (2) and (3) to compute the reachable sets takes a lot of time and even impossible to solve for high-dimensional systems [11]. The approximated computation of the reachable sets, proposed in the next section, alleviates those limitations without violating the guarantees on safety.

III. Ellipsoidal Reachable Sets

Instead of directly solving the original HJ PDEs, we tackle the reachability problem in a different direction using the generalized Hopf formula [13]. This formula provides solutions of the HJ PDEs for the following class of system:

$$\dot{z}(t) = f_z(w(t)),$$

where $z \in \mathbb{R}^{n_x}$ the coordinate-transformed state vector. Since the system of our interest (1) is different from the above one, we first transform the closed-loop system to utilize the generalized Hopf formula.

A. Coordinate Transformation

Given the initial guess on $x_r(t)$, we can compute a disturbance-free state trajectory $\vec{q}_x(t) \in \mathbb{R}^{n_x}$ by solving a differential equation $\dot{\vec{q}}_x(t) = g(\vec{q}_x(t), x_r(t), 0)$ with the initial condition $\vec{q}_x(t_0) = q_0$. We linearize (1) along $\vec{q}_x(t)$ and $x_r(t)$ to construct a linear time-varying (LTV) system as follows:

$$\begin{aligned} \dot{x}(t) &= A(t)x(t) + D(t)w(t) + r(t), \\ \begin{cases} A(t) &= \frac{\partial g}{\partial x}\big|_{(\vec{q}_x(t), x_r(t), 0)} \in \mathbb{R}^{n_x \times n_x} \\ D(t) &= \frac{\partial g}{\partial w}\big|_{(\vec{q}_x(t), x_r(t), 0)} \in \mathbb{R}^{n_x \times n_w} \\ r(t) &= g(\vec{q}_x(t), x_r(t), 0) - A(t)\vec{q}_x(t) \in \mathbb{R}^{n_x} \end{cases} \end{aligned} . \tag{5}$$

We assume that the linearization error is negligible, but nonlinearity bounders [7] or interval analysis [14] can be used for relieving the assumption. The LTV system (5) can further be transformed with $x(t) = P(t)z(t)$, where $P(t) \in \mathbb{R}^{n_x \times n_x}$ is the fundamental matrix of a homogenous system $\dot{x}(t) = A(t)x(t)$. The system equation in the z coordinate is

$$\begin{aligned} \dot{z}(t) &= P(t)^{-1}D(t)w(t) + P(t)^{-1}r(t) \\ &= D_z(t)w(t) + r_z(t). \end{aligned} \tag{6}$$

This transformation can also be applied backward in time. Given the same initial guess on $x_r(t)$, we can compute a trajectory $\overleftarrow{q}_x(t) \in \mathbb{R}^{n_x}$ by the backward integration of the dynamics with the terminal condition $\overleftarrow{q}_x(t_f) = q_f$. The LTV system linearized along $\overleftarrow{q}_x(t)$ and $x_r(t)$ is used for the backward reachability analysis, and we omit the detail.

Based on the transformation (6), the forward reachability problem (2) can be converted to the z coordinate as follows:

$$\begin{cases} \dfrac{\partial V_z^{FRS}}{\partial t} + H_z^{FRS}\left(\dfrac{\partial V_z^{FRS}}{\partial z}, t\right) = 0 \\ V_z^{FRS}(z, t_0) = l_{0,z}(z) \\ H_z^{FRS}(p,t) = \max\limits_{w \in \mathbb{W}} \big(p \cdot \dot{z}(t)\big) \end{cases} .$$

The subscript z represents the corresponding value or function expressed in the z coordinate. For instance, $l_{0,z}(z) = l_0(z)$ since $x(t_0) = z(t_0)$. Due to the transformation (6), the Hamiltonian in the z coordinate no longer depends on the state variable. Thus, the Hamiltonian can be computed as

$$H_z^{FRS}(p,t) = p^\top r_z(t) + p^\top D_z(t) w_m + \sum_{i=1}^{n_w} |p^\top D_{z,i}(t)| w_{M,i},$$

with the optimal disturbance

$$w^\star(t) = w_m + \mathrm{diag}\big(\mathrm{sign}(p^\top D_z(t))\big) w_M,$$

where $D_{z,i}(t)$ and $w_{M,i}$ are the i-th column and element of $D_z(t)$ and $w_{M,i}$ respectively.

For the backward reachability problem, we introduce a change of variable $s = t_0 + t_f - t$ [15] and define a new state vector $y(s) = z(t)$ to convert the final value PDE to the initial value PDE. The dynamics in time backward is written as

$$\begin{aligned} \dot{y}(s) &= -D_z(t_0 + t_f - s)w(t_0 + t_f - s) - r_z(t_0 + t_f - s) \\ &= D_y(s)w(t_0 + t_f - s) + r_y(s). \end{aligned}$$

Finally, the backward reachability problem (3) is

$$\begin{cases} \dfrac{\partial V_y^{BRS}}{\partial s} + H_y^{BRS}\left(\dfrac{\partial V_y^{BRS}}{\partial y}, s\right) = 0 \\ V_y^{BRS}(y, t_0) = l_{f,y}(y) \\ H_y^{BRS}(p,s) = \min\limits_{w \in \mathbb{W}} \big(p \cdot \dot{y}(s)\big) \end{cases} , \tag{7}$$

where $l_{f,y}(y) = l_f(P(t_f)y)$ since $x(t_f) = P(t_f)y(t_0)$. The Hamiltonian is computed as

$$H_y^{BRS}(p,s) = p^\top r_y(s) + p^\top D_y(s) w_m - \sum_{i=1}^{n_w} |p^\top D_{y,i}(s)| w_{M,i},$$

with the optimal disturbance

$$w^\star(t_0 + t_f - s) = w_m - \mathrm{diag}\big(\mathrm{sign}(p^\top D_y(s))\big) w_M,$$

where $D_{y,i}(s)$ is the i-th column of $D_y(s)$.

B. Analytic Expression for Reachable Sets

This section aims to characterize the zero level set of the value functions $V_z^{FRS}(z,t)$ and $V_y^{BRS}(y,s)$. We specify the initial and target sets as the following ellipsoids:

$$\mathcal{X}_0 = \mathcal{E}(q_0, Q_0), \quad \mathcal{X}_f = \mathcal{E}(q_f, Q_f),$$

where $\mathcal{E}(q,Q) = \{q + Q^{1/2} v \,|\, \|v\|_2^2 \le 1\}$ is the set of points in an ellipsoid with the center $q \in \mathbb{R}^{n_x}$ and shape matrix $Q \in \mathbb{S}_{++}^{n_x}$. Consequently, the initial and final value functions in the x coordinate can be expressed as

$$l_0(x) = (x - q_0)^\top Q_0^{-1} (x - q_0) - 1,$$
$$l_f(x) = (x - q_f)^\top Q_f^{-1} (x - q_f) - 1.$$

Proposition. The zero level set of $V_y^{BRS}(y,s)$ is

$$\mathcal{Y}(s) = \mathcal{E}(q_y(s), Q_{f,y}) \ominus \mathcal{D}_y(s), \tag{8}$$

where

$$q_y(s) = P(t_f)^{-1} q_f + \int_{t_0}^{s} r_y(\tau) d\tau,$$
$$Q_{f,y} = P(t_f)^{-1} Q_f P(t_f)^{-\top},$$
$$\mathcal{D}_y(s) = -\int_{t_0}^{s} D_y(\tau) w_m d\tau + \bigoplus_{i=1}^{n_w} \mathcal{D}_{y,i}(s),$$
$$\mathcal{D}_{y,i}(s) = \left\{ \int_{t_0}^{s} D_{y,i}(\tau) w_{M,i} \mathrm{sign}\left(D_{y,i}(\tau)^\top v\right) d\tau \,\middle|\, \|v\|_{Q_{f,y}}^2 \le 1 \right\}.$$

Proof. We first derive the initial value $l_{f,y}(y)$ in (7) as

$$\begin{aligned} l_{f,y}(y) &= (P(t_f)y - q_f)^\top Q_f^{-1} (P(t_f)y - q_f) \\ &= (y - q_{f,y})^\top Q_{f,y}^{-1} (y - q_{f,y}), \end{aligned}$$

where $q_{f,y} = P(t_f)^{-1} q_f$. The generalized Hopf formula for (7) yields

$$\begin{cases} V_y^{BRS}(y,s) & = -\min_p \big(-y \cdot p + W_y^{BRS}(p,s) \big) \\ W_y^{BRS}(p,s) & = h_{f,y}(p) + \int_{t_0}^{s} H_y^{BRS}(p,\tau) d\tau \\ h_{f,y}(p) & = \max_y \big(y \cdot p - l_{f,y}(y) \big) \end{cases}.$$

States along the boundary of the zero level set of $V_y^{BRS}(y,s)$ must satisfy the following:

$$V_y^{BRS}(y,s) = \min_p \big(-y \cdot p + W_y^{BRS}(p,s) \big) = 0. \tag{9}$$

To find the expression of y, we use the property of Fenchel-Legendre transform [16] that the derivative of a convex function is the optimal argument of its conjugate as in [12]. Let $p^\star \in \mathbb{R}^{n_x}$ be the optimal argument of (9). From the first-order optimality condition, we get

$$\begin{aligned} y^\star(s) &= y(s; p^\star) \\ &= \frac{\partial}{\partial p} W_y^{BRS}(p,s)\Big|_{p=p^\star} \\ &= \frac{\partial h_{f,y}(p)}{\partial p}\Big|_{p=p^\star} + \int_{t_0}^{s} \frac{\partial H_y^{BRS}(p,\tau)}{\partial p}\Big|_{p=p^\star} d\tau. \end{aligned} \tag{10}$$

By replacing (9) with (10), V_y^{BRS} can be expressed with $p^\star$:

$$V_y^{BRS}(p^\star, s) = \frac{1}{4} p^{\star\top} Q_{f,y} p^\star - 1, \tag{11}$$

provided that

$$\frac{\partial h_{f,y}(p)}{\partial p}\Big|_{p=p^\star} = \frac{1}{2} Q_{f,y} p^\star + q_{f,y},$$
$$\frac{\partial H_y^{BRS}(p,\tau)}{\partial p}\Big|_{p=p^\star} = r_y(\tau) + D_y(\tau) w_m - \sum_{i=1}^{n_w} D_{y,i}(\tau) w_{M,i} \mathrm{sign}\big(D_{y,i}(\tau)^\top p^\star\big).$$

The subzero level set of (11) is $p^\star \in \big\{ 2 Q_{f,y}^{-\frac{1}{2}} v \,\big|\, \|v\|_2^2 \le 1 \big\}$. Consequently, we get an analytic expression for the backward reachable set from (10) as

$$\mathcal{Y}(t) = \left\{ \begin{array}{l} q_{f,y} + Q_{f,y} v + \int_{t_0}^{s} \big(r_y(\tau) + D_y(\tau) w_m \big) d\tau \\ - \sum_{i=1}^{n_w} \int_{t_0}^{s} D_{y,i}(\tau) w_{M,i} \mathrm{sign}\left(D_{y,i}(\tau)^\top v \right) d\tau \end{array} \right\},$$

for all $\|v\|_{Q_{f,y}}^2 \le 1$. The set above is the Minkowski difference of the disturbance-free set $\mathcal{E}(q_y(s), Q_{f,y})$ and the set due to disturbance $\mathcal{D}_y(s)$. □

The zero level set of $V_z^{FRS}(z,t)$ is characterized as

$$\mathcal{Z}(t) = \mathcal{E}(q_z(t), Q_0) \oplus \mathcal{D}_z(t), \tag{12}$$

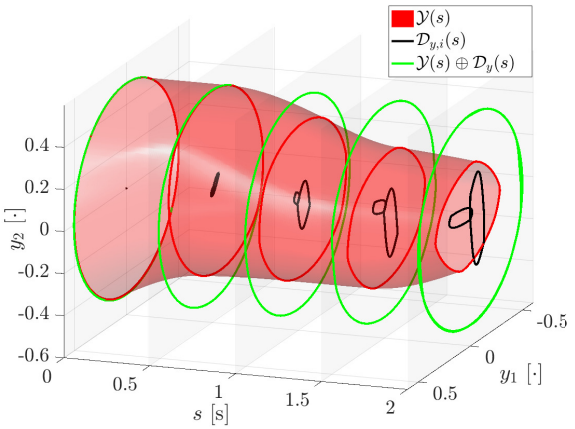

Fig. 2. Backward reachable sets of a 2-state LTV system: $\dot{z}_1(t) = 2\cos(t) w_1(t) - t^2 w_2(t)$, $\dot{z}_2(t) = 0.4 t w_1(t) + 7\cos(3t) w_2(t)$ with $\bar{w} = [0.0, 0.0]^\top$, $\underline{w} = [-0.1, -0.05]^\top$, $q_f = [0,0]^\top$, and $Q_f = \mathrm{diag}([0.25, 0.25])$. Note that $P(t) = I_{n_x}$ for this system. Red surface describes the true reachable sets. Black lines represent regions due to disturbances. Green lines are the Minkowski sum of $\mathcal{Y}(s)$ and $\mathcal{D}_y(s)$.

where

$$q_z(t) = q_0 + \int_{t_0}^{t} r_z(\tau) d\tau,$$

$$\mathcal{D}_z(t) = \int_{t_0}^{t} D_z(\tau) w_m d\tau + \bigoplus_{i=1}^{n_w} \mathcal{D}_{z,i}(t),$$

$$\mathcal{D}_{z,i}(t) = \left\{ \int_{t_0}^{t} D_{z,i}(\tau) w_{M,i} \text{sign}\left(D_{z,i}(\tau)^\top v \right) d\tau \middle| \|v\|_{Q_0}^2 \leq 1 \right\}.$$

For more details of the analytic expression for the forward reachable set, please see [12].

Fig. 2 illustrates how the backward reachable sets are constructed. We use the level set toolbox [17] to compute $\mathcal{Y}(s)$. As time goes backward (which means the increase in s), the size of $\mathcal{D}_{y,i}(s)$ is increased. The Minkowski sum of $\mathcal{Y}(s)$ and $\mathcal{D}_y(s)$ is identical with the target set $\mathcal{E}(q_y(s), Q_{f,y})$ for all time, which validates the proposition (8).

C. Ellipsoidal Approximation

The derived expressions for the reachable sets so far may not be appropriate for robust trajectory planning, because numerical computation of the Minkowski sum and difference becomes intractable as the number of state and disturbance increase. We alleviate this computational issue by approximating the true reachable sets as ellipsoids. The disturbance-free sets in (8) and (12) are already ellipsoids. Thus, we focus on the sets due to disturbance, namely $\mathcal{D}_z(t)$ and $\mathcal{D}_y(s)$.

In approximating $\mathcal{D}_z(t)$ and $\mathcal{D}_y(s)$, the guarantees on the safety and reachability to the target set must not be violated. Considering the characteristics of the forward and backward reachable sets, $\mathcal{D}_z(t)$ and $\mathcal{D}_y(s)$ should be conservatively approximated. If the approximation on $\mathcal{D}_z(t)$ underestimates the true set, the system can exceed the approximated forward reachable sets, which means that the safety guarantee no longer holds. Similarly, overestimated backward reachable sets are computed if the approximation on $\mathcal{D}_y(s)$ does not fully cover the true set. The system may not reach the target set when it starts from the overly approximated backward reachable set.

We utilize the method proposed in [12] which produces a conservative and compact ellipsoidal approximation on the set due to disturbance. We briefly summarize the resultant ellipsoids as follows:

$$\mathcal{D}_z(t) \subseteq \mathcal{E}(b_z(t), B_z(t)), \quad \mathcal{D}_y(s) \subseteq \mathcal{E}(b_y(s), B_y(s)),$$

where $b_z(t) = \int_{t_0}^{t} D_z(\tau) w_m d\tau$, $b_y(s) = -\int_{t_0}^{s} D_y(\tau) w_m d\tau$, and

$$B_{z,i}(t) = (t - t_0) w_{M,i}^2 \int_{t_0}^{t} \left(D_{z,i}(\tau) D_{z,i}(\tau)^\top + \varepsilon I_{n_x} \right) d\tau,$$

$$B_z(t) = \bigoplus_{i=1}^{n_w} B_{z,i}(t),$$

$$B_{y,i}(s) = (s - t_0) w_{M,i}^2 \int_{t_0}^{s} \left(D_{y,i}(\tau) D_{y,i}(\tau)^\top + \varepsilon I_{n_x} \right) d\tau,$$

$$B_y(s) = \bigoplus_{i=1}^{n_w} B_{y,i}(s),$$

with an arbitrarily small positive scalar ε. Note that the operator $\oplus$ for the shape matrices represents

$$\bigoplus_{i=1}^{n_w} B_{z,i}(t) = \min_{\alpha} \text{trace} \sum_{i=1}^{n_w} \frac{B_{z,i}(t)}{\alpha_i},$$

$$\text{s.t.} \quad \sum_{i=1}^{n_w} \alpha_i = 1, \quad \alpha_i > 0, \quad \alpha \in \mathbb{R}^{n_w},$$

allowing some notation abuse. The trace criterion is used for the Minkowski sum of ellipsoids [18]. Also, $B_{z,i}(t)$ and $B_{y,i}(s)$ can be computed by solving Lyapunov equations as discussed in [12].

The true forward reachable set $\mathcal{Z}(t)$ is approximated as

$$\mathcal{Z}(t) \subseteq \mathcal{E}(q_z(t) + b_z(t), Q_z(t)),$$
$$Q_z(t) = Q_0 \oplus B_z(t).$$

For the backward reachable sets, we utilize the maximal internal approximation on the Minkowski difference of ellipsoids [19]. The approximated ellipsoid for $\mathcal{Y}(s)$ is

$$\mathcal{E}(q_y(s) + b_y(s), Q_y(s)) \subseteq \mathcal{Y}(s),$$
$$Q_y(s) = Q_{f,y} \ominus B_y(s),$$

where the operator $\ominus$ for the shape matrices represents

$$Q_{f,y} \ominus B_y(s) = \max_{a_1, a_2} \text{trace}\left(Q_{f,y}/a_1 + B_y(s)/a_2 \right),$$
$$\text{s.t.} \quad a_1 + a_2 = 1, \quad a_1 > 1, \quad a_2 < 0,$$

provided that $\mathcal{E}(0, B_y(s)) \subseteq \mathcal{E}(0, Q_{f,y})$. Note that the trace criterion is used to compute the Minkowski difference of ellipsoids for computational simplicity.

Finally, the ellipsoidal reachable sets in the original coordinate are computed. Considering the coordinate transform $x(t) = P(t)z(t)$, the ellipsoid which compactly encloses the forward reachable set is

$$\vec{\mathcal{X}}(t_0, t) \subseteq \mathcal{E}(\vec{q}_x(t) + \vec{b}_x(t), \vec{Q}_x(t)),$$
$$\vec{b}_x(t) = P(t) b_z(t), \tag{13}$$
$$\vec{Q}_x(t) = P(t) Q_z(t) P(t)^\top.$$

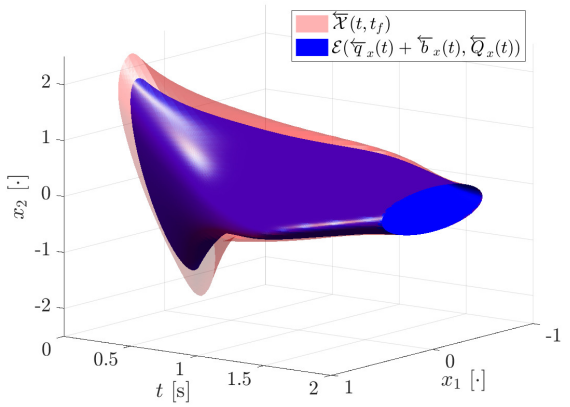

Fig. 3. Ellipsoidal approximation on the backward reachable sets for a 2-state LTV system: $\dot{x}_1(t) = (-0.8t + 0.5)x_1(t) + \cos(1.5t + 2)x_2(t) + 2\cos(t)w_1(t) - t^2 w_2(t)$, $\dot{x}_2(t) = 0.5t^{2/3}x_1(t) - 2\exp(-0.7t)x_2(t) + 0.4t w_1(t) + 7\cos(3t)w_2(t)$ with $\bar{w} = [0.07, 0.07]^\top$, $\underline{w} = [-0.035, -0.035]^\top$, $q_f = [0, 0]^\top$, and $Q_f = \text{diag}([0.25, 0.16])$. Red region is the true reachable set, and blue shape is the proposed approximation.

Note that the center of the disturbance-free set, namely $\vec{q}_x(t)$, is already computed before constructing the LTV system (5). Similarly, the maximal ellipsoid that fits inside of the backward reachable set is

$$\begin{aligned} &\mathcal{E}(\overleftarrow{q}_x(t)+\overleftarrow{b}_x(t),\overleftarrow{Q}_x(t)) \subseteq \overleftarrow{\mathcal{X}}(t,t_f), \\ &\overleftarrow{b}_x(t) = P(t)b_y(t_0+t_f-t), \\ &\overleftarrow{Q}_x(t) = P(t)Q_y(t_0+t_f-t)P(t)^\top, \end{aligned} \tag{14}$$

with the change of variable $s = t_0 + t_f - t$.

Results of the ellipsoidal approximation are illustrated in Fig. 3. We compare the proposed approximation and the true backward reachable sets which are computed by the level set toolbox [17]. As expected, the resultant ellipsoids are always located inside of the true set for all time. If the approximation overestimates the true backward reachable sets, it means that some states in the approximated sets may not reach the target set. Thus, the proposed approximation (showing slight underestimation) is valid for guaranteeing the reachability to the target set. With the proposed approximations (13) and (14), the original trajectory planning problem (4) becomes tractable. The details of the trajectory optimization will be covered in the following section.

IV. Robust Trajectory Planning

A. Cost and Constraints

Let $x_g(t) \in \mathbb{R}^{n_x}$ be the initial guess for the reference trajectory for $t \in [t_0, t_f]$. The initial guess, for instance, can be a straight line which connects the initial state q_0 and the target state q_f. We simply use the cost function of the trajectory optimization (4) as

$$L(x_r(t)) = (x_r(t) - x_g(t))^2,$$

which makes the planned trajectory follow the initial guess in the absence of obstacles.

For avoiding a collision, we compute the distance between the ellipsoidal reachable sets and the obstacles. We consider the obstacle regions as ellipsoids $\mathcal{E}(q_{obs}, Q_{obs})$, where $q_{obs} \in \mathbb{R}^{n_x}$ and $Q_{obs} \in \mathbb{S}^{n_x}_{++}$ are the position and shape matrix of the obstacle. We use the collision avoidance constraint [12] as

$$c(\vec{q}_x(t)) = \|\vec{q}_x(t) + \vec{b}_x(t) - q_{obs}\|^2_{(\vec{Q}_x(t) \oplus Q_{obs})^{-1}} - 1.$$

The case for the ellipsoidal backward reachable sets can be considered similarly.

The constraint for the reachability to the target set is constructed as follows. We compute the Minkowski difference of $\mathcal{E}(\vec{q}_x(t_c), \vec{Q}_x(t_c))$ and $\mathcal{E}(\overleftarrow{q}_x(t_c), \overleftarrow{Q}_x(t_c))$. To enforce that the forward reachable set must be contained in the backward reachable set, the Minkowski difference of the two ellipsoids should not contain the origin. Thus, we use

$$(\vec{q}_x(t_c) - \overleftarrow{q}_x(t_c))^\top (\vec{Q}_x(t_c) \ominus \overleftarrow{Q}_x(t_c))^{-1} (\vec{q}_x(t_c) - \overleftarrow{q}_x(t_c)) > 1$$

as the constraint for the reachability to the target set.

Note that $\vec{b}_x(t)$, $\vec{Q}_x(t)$, $\overleftarrow{b}_x(t)$ and $\overleftarrow{Q}_x(t)$ in the constraints are fixed until $x_r(t)$ is updated. It is possible because the ellipsoidal reachable sets can be computed independently of the trajectory optimization procedure. After we update $x_r(t)$ based on the optimization result, we reevaluate the ellipsoidal reachable sets since the linearization points are different from the previous one. Then, we solve the optimization problem again and repeat the process until the optimal reference trajectory converges.

B. Simulation Results

Fig. 1 illustrates the result of the robust trajectory planning for the multirotor dynamics from [9]. The parameters used in the simulation is detailed in Table I. We utilize the constrained version of differential dynamic programming (DDP) [20] to solve the nonlinear optimization problem (4). The reference trajectory is generated so that the ellipsoidal reachable sets do not intersect with the obstacle regions. At the same time, the system can pass through narrow gaps between the obstacles. Due to the constraint related with the backward reachable sets, the reference trajectory is automatically adjusted near the target set. We can also confirm that all the states passing through the beginning of the backward reachable set eventually traverse the target set without exceeding the backward reachable sets (zoom-in figure at the corner of Fig. 1).

V. Conclusion

This paper proposes a robust trajectory planning algorithm with a simultaneous guarantee on the safety and the reachability to the target set. We characterize the forward and backward reachable sets of the closed-loop dynamics of the multirotor using the Hamilton-Jacobi reachability analysis. We approximate the reachable sets as ellipsoids and formulate a tractable robust trajectory planning problem with the ellipsoidal reachable sets. Our approximation on the reachable sets is based on the analytic solution of the HJ PDE and does not require any optimization. Thus, it becomes possible to perform reachability analysis in a computationally efficient way. Also, the proposed planning algorithm ensures safety and reachability by considering the forward and backward reachable sets in a unified way. The simulation result of a multirotor traversing a narrow gap without collision validates the effectiveness of the proposed planning algorithm.

TABLE I

Parameters for the robust planning simulation

Parameter	Value	Description
q_0	$[-1.5\text{m}, -1\text{m}, 1\text{m}, 0, 0, 0, 0, 0, 0]^\top$	Center of the initial set
q_f	$[0, 0, 1\text{m}, 1\text{m/s}, 0, 0, 10\text{deg}, 0, 0]^\top$	Center of the target set
Q_0	$\text{diag}([0.1\text{m}, 0.1\text{m}, 0.1\text{m}, 0.1\text{m/s}, 0.1\text{m/s}, 0.1\text{m/s}, 5\text{deg}, 5\text{deg}, 5\text{deg}])^2$	Shape of the initial set
Q_f	$\text{diag}([0.1\text{m}, 0.1\text{m}, 0.1\text{m}, 0.1\text{m/s}, 0.1\text{m/s}, 0.1\text{m/s}, 10\text{deg}, 10\text{deg}, 10\text{deg}])^2$	Shape of the target set
$\lvert\delta\mathbf{p}\rvert$	$[0.005\text{m}, 0.005\text{m}, 0.005\text{m}]^\top$	Position measurement noise
$\lvert\delta\mathbf{v}\rvert$	$[0.001\text{m/s}, 0.001\text{m/s}, 0.001\text{m/s}]^\top$	Velocity measurement noise
$\lvert\delta\Phi\rvert$	$[0.01\text{deg}, 0.01\text{deg}, 0.01\text{deg}]^\top$	Attitude measurement noise
$\lvert\Delta\rvert$	$[0.1\text{N}, 0.1\text{N}, 0.1\text{N}]^\top$	External force bound
K	$[6, 6, 7, 4, 4, 5, 5, 5, 5]^\top$	Feedback gains
m	2kg	Mass of the multirotor
t_f	2.1s	Time of the target set
t_c	1.8s	Time when the FRS and BRS meet

REFERENCES

[1] Ian M Mitchell, Alexandre M Bayen, and Claire J Tomlin. A time-dependent hamilton-jacobi formulation of reachable sets for continuous dynamic games. *IEEE Transactions on automatic control*, 50(7):947–957, 2005.

[2] Anirudha Majumdar and Russ Tedrake. Funnel libraries for real-time robust feedback motion planning. *The International Journal of Robotics Research*, 36(8):947–982, 2017.

[3] Suseong Kim, Davide Falanga, and Davide Scaramuzza. Computing the forward reachable set for a multirotor under first-order aerodynamic effects. *IEEE Robotics and Automation Letters*, 3(4):2934–2941, 2018.

[4] Sylvia L Herbert, Mo Chen, SooJean Han, Somil Bansal, Jaime F Fisac, and Claire J Tomlin. Fastrack: a modular framework for fast and guaranteed safe motion planning. In *Decision and Control (CDC), 2017 IEEE 56th Annual Conference on*, pages 1517–1522. IEEE, 2017.

[5] David Fridovich-Keil, Sylvia L Herbert, Jaime F Fisac, Sampada Deglurkar, and Claire J Tomlin. Planning, fast and slow: A framework for adaptive real-time safe trajectory planning. In *2018 IEEE International Conference on Robotics and Automation (ICRA)*, pages 387–394. IEEE, 2018.

[6] Mario E Villanueva, Boris Houska, and Benoît Chachuat. Unified framework for the propagation of continuous-time enclosures for parametric nonlinear odes. *Journal of Global Optimization*, 62(3):575–613, 2015.

[7] Mario E Villanueva, Rien Quirynen, Moritz Diehl, Benoît Chachuat, and Boris Houska. Robust mpc via min–max differential inequalities. *Automatica*, 77:311–321, 2017.

[8] Gowtham Garimella, Matthew Sheckells, Joseph L Moore, and Marin Kobilarov. Robust obstacle avoidance using tube nmpc. In *Robotics: Science and Systems*, 2018.

[9] Taeyoung Lee, Melvin Leoky, and N Harris McClamroch. Geometric tracking control of a quadrotor uav on se (3). In *Decision and Control (CDC), 2010 49th IEEE Conference on*, pages 5420–5425. IEEE, 2010.

[10] Somil Bansal, Mo Chen, Sylvia Herbert, and Claire J Tomlin. Hamilton-jacobi reachability: A brief overview and recent advances. In *Decision and Control (CDC), 2017 IEEE 56th Annual Conference on*, pages 2242–2253. IEEE, 2017.

[11] Jérôme Darbon and Stanley Osher. Algorithms for overcoming the curse of dimensionality for certain hamilton–jacobi equations arising in control theory and elsewhere. *Research in the Mathematical Sciences*, 3(1):19, 2016.

[12] Hoseong Seo, Donggun Lee, Clark Youngdong Son, Claire J Tomlin, and H Jin Kim. Robust trajectory planning for a multirotor against disturbance based on hamilton-jacobi reachability analysis. In *2019 IEEE/RSJ International Conference on Intelligent Robots and Systems (IROS)*, pages 3150–3157. IEEE, 2019.

[13] P-L Lions and J-C Rochet. Hopf formula and multitime hamilton-jacobi equations. *Proceedings of the American Mathematical Society*, 96(1):79–84, 1986.

[14] Matthias Althoff, Olaf Stursberg, and Martin Buss. Reachability analysis of nonlinear systems with uncertain parameters using conservative linearization. In *2008 47th IEEE Conference on Decision and Control*, pages 4042–4048. IEEE, 2008.

[15] Matthew R Kirchner, Robert Mar, Gary Hewer, Jérôme Darbon, Stanley Osher, and Yat Tin Chow. Time-optimal collaborative guidance using the generalized hopf formula. *IEEE Control Systems Letters*, 2(2):201–206, 2018.

[16] Jérôme Darbon. On convex finite-dimensional variational methods in imaging sciences and hamilton–jacobi equations. *SIAM Journal on Imaging Sciences*, 8(4):2268–2293, 2015.

[17] Ian M Mitchell. The flexible, extensible and efficient toolbox of level set methods. *Journal of Scientific Computing*, 35(2-3):300–329, 2008.

[18] AB Kurzhanski and TF Filippova. On the theory of trajectory tubes—a mathematical formalism for uncertain dynamics, viability and control. In *Advances in nonlinear dynamics and control: a report from Russia*, pages 122–188. Springer, 1993.

[19] AB Kurzhanskii and Istvan Vályi. Ellipsoidal calculus for estimation and control. 1997.

[20] Brian Plancher, Zachary Manchester, and Scott Kuindersma. Constrained unscented dynamic programming. In *2017 IEEE/RSJ International Conference on Intelligent Robots and Systems (IROS)*, pages 5674–5680. IEEE, 2017.